

The C₇H₁₀ Potential Energy Landscape: Concerted Transition States and Diradical Intermediates for the Retro-Diels–Alder Reaction and [1,3] Sigmatropic Shifts of Norbornene

Brett R. Beno, Sarah Wilsey, and K. N. Houk*

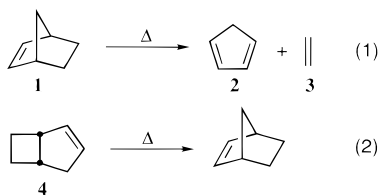
Contribution from the Department of Chemistry and Biochemistry, University of California, Los Angeles, California 90095-1569

Received May 26, 1998. Revised Manuscript Received February 15, 1999

Abstract: The potential energy surfaces for the thermal reactions of bicyclo[3.2.0]hept-2-ene and norbornene have been explored with density functional theory at the Becke3LYP/6-31G* level. Both concerted and diradical pathways for the retro-Diels–Alder reaction of norbornene have been examined, and the activation parameters and ¹³C primary kinetic isotope effects predicted for the concerted pathway are in excellent agreement with experimental data. The concerted mechanism is favored over the lowest energy stepwise diradical route by 12.4 kcal/mol. For the orbital symmetry-allowed suprafacial-inversion (*si*) pathway of the [1,3] sigmatropic rearrangement of bicyclo[3.2.0]hept-2-ene to form norbornene, a mechanism involving a transition state which leads to a broad diradical plateau on the potential energy surface is predicted. Implications of these surfaces, which differ substantially from those obtained by semiempirical calculations, are also discussed.

Introduction

Norbornene (**1**) and the isomeric molecules of formula C₇H₁₀ have provided the proving ground for a number of classic mechanistic problems in organic chemistry, particularly those which test the scope and limitations of the Woodward–Hoffmann rules.¹ Is the retro-Diels–Alder reaction of norbornene (eq 1) concerted or stepwise? Is the [1,3] shift of bicyclo[3.2.0]hept-2-ene (**4**) to give norbornene (eq 2) concerted, subject to Woodward–Hoffmann control,^{1a} or if that route is blocked, controlled by Berson’s “subjacent orbital” control?² Does this reaction also involve diradical intermediates?³



These reactions are an intriguing complement, since they could involve a common intermediate. The recent femtosecond kinetic studies of the retro-Diels–Alder reaction of norbornene by Zewail have focused additional attention on this reaction.⁴ Carpenter’s dynamics simulation⁵ for the [1,3] sigmatropic

rearrangement of bicyclo[3.2.0]heptene to form norbornene, a reaction which has been studied experimentally in detail by Berson et al.,⁶ also stimulated our study of the details of the potential energy surfaces.

This paper is organized in the following manner. First, previous experimental and theoretical work on the retro-Diels–Alder reaction of **1** and the [1,3] sigmatropic rearrangement of **4** are summarized. This is followed by a brief description of the computational techniques employed in the present study. Finally, the Becke3LYP/6-31G* results for the retro-Diels–Alder and [1,3] sigmatropic shift reactions are presented, and the mechanistic details of both reactions are discussed.

Background

The Norbornene Retro-Diels–Alder Reaction. Both a synchronous concerted mechanism and stepwise diradical pathways involving anti intermediates (denoted anti and gauche-out in Figure 1) are possible for the retro-Diels–Alder reaction of **1** [eq 1]. Activation parameters for this reaction have been determined by several groups.⁷ The values of ΔH^\ddagger and ΔS^\ddagger are 43.5 kcal/mol and 3.5 eu, respectively.⁸ ΔH_{rxn} is 23.2 ± 0.6 kcal/mol.⁹ The small positive ΔS^\ddagger implies a highly ordered transition state and is consistent with either a concerted mechanism or a diradical mechanism in which only one of the C–C bonds has broken to a significant extent in the transition state. Using group additivity calculations, Benson estimated a ΔH_{rxn} of 48 kcal/mol for the formation of a diradical intermediate from norbornene.¹⁰ This is 4.5 kcal/mol larger than the

(1) (a) Woodward, R. B.; Hoffmann, R. *The Conservation of Orbital Symmetry*; Verlag Chemie: Weinheim, 1970. (b) Fleming, I. *Frontier Orbitals and Organic Chemical Reactions*; John Wiley & Sons: New York, 1976.

(2) Berson, J. A.; Salem, L. *J. Am. Chem. Soc.* **1972**, *94*, 8917.

(3) (a) Klärner, F.-G.; Drewes, R.; Hasselmann, D. *J. Am. Chem. Soc.* **1988**, *110*, 297. (b) Newman-Evans, R. H.; Carpenter, B. K. *J. Am. Chem. Soc.* **1984**, *106*, 7994.

(4) Horn, B. A.; Herek, J. L.; Zewail, A. H. *J. Am. Chem. Soc.* **1996**, *118*, 8755.

(5) (a) Carpenter, B. K. *J. Am. Chem. Soc.* **1995**, *117*, 6336. (b) Carpenter, B. K. *J. Am. Chem. Soc.* **1996**, *118*, 10329. (c) For a lucid overview of this and other reactions of this type subject to dynamic control, see: Carpenter, B. K. *Angew. Chem., Int. Ed.* **1998**, *37*, 3340.

(6) (a) Berson, J. A.; Holder, R. W. *J. Am. Chem. Soc.* **1973**, *95*, 2037. (b) Berson, J. A. *Acc. Chem. Res.* **1972**, *5*, 406.

(7) (a) Walsh, R.; Wells, J. M. *J. Chem. Soc., Perkin Trans. 2* **1976**, 52. (b) Roquette, B. C. *J. Phys. Chem.* **1965**, *69*, 1351. (c) Herndon, W. C.; Cooper, W. B., Jr.; Chambers, M. J. *J. Phys. Chem.* **1964**, *68*, 2016.

(8) Determined from raw data from ref 7a.

(9) Walsh, R.; Wells, J. M. *J. Chem. Thermodyn.* **1976**, *8*, 55.

(10) Benson, S. W. *Thermochemical Kinetics*; John Wiley & Sons: New York, 1976; pp 131–132.

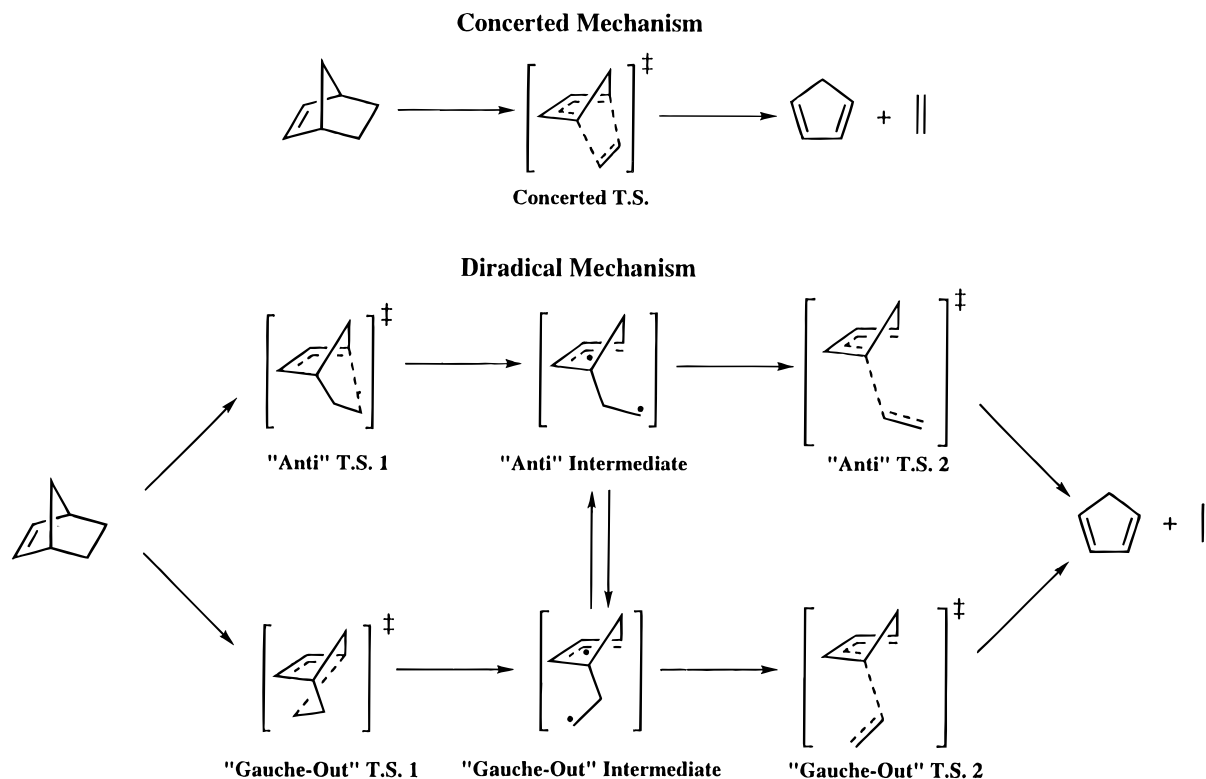
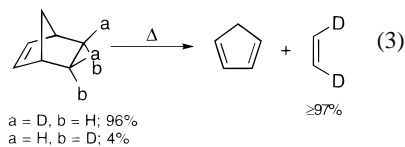


Figure 1. Concerted and stepwise diradical pathways of the retro-Diels–Alder reaction of norbornene.

measured ΔH^\ddagger for the reaction. Thus, experimental evidence suggests that the concerted pathway is favored over a diradical mechanism by at least 4.5 kcal/mol. This is Doering's "energy of concert."¹¹

High stereoselectivity has been demonstrated for the retro-Diels–Alder reaction of **1**. The thermolysis of dideuterated **1** (320 °C), studied by Klärner et al., resulted in the formation of $\geq 97\%$ (*Z*)-1,2-dideuterioethene (eq 3). The reaction is completely stereoselective within the limits of detection of the experiment.^{3a}



There has been much excitement recently about the direct observation of transition states and short-lived intermediates in reactions.¹² Zewail utilized⁴ femtosecond laser spectroscopy with mass spectrometric detection to study the retro-Diels–Alder reaction of norbornene. An intermediate with the mass of norbornene appears with the laser pulse and decays in 160 ± 15 fs. The rise and decay times for a second intermediate with the mass of cyclopentadiene were 30 ± 5 fs and 220 ± 20 fs, respectively. Since the rise time for the cyclopentadiene species and the decay time for the norbornene species differ, Zewail proposed that the reaction occurs via two mechanisms. The 66 amu intermediate was postulated to be a vibrationally excited cyclopent-2-ene-1,4-diyl species formed from concerted breakage of two C–C bonds in norbornene, whereas the 94 amu intermediate was presumed to be a diradical formed in a

stepwise retro-Diels–Alder process. Stereochemical retention was predicted for both the concerted and diradical pathways since the mass 94 amu intermediate disappears in 160 fs, which is less than the rotational period of a C–C bond in ethane (1–10 ps).⁴ To fully understand the laser-induced decomposition, both the excited- and ground-state surfaces must be explored with CASSCF theory; such studies will be reported in due course.¹³ Here we explore the ground-state reactions of norbornene and isomeric C₇H₁₀ species with B3LYP theory.

Previous theoretical studies have been limited to the concerted mechanism of the Diels–Alder cycloaddition of **2** and **3** to form **1**.¹⁴ Very few of these report energies for **1** which are required to determine the activation barrier for the retro-Diels–Alder reaction. At the AM1 and RHF/3-21G levels of theory, which neglect electron correlation, the activation barrier of the retro-Diels–Alder reaction is overestimated by 13 and 19 kcal/mol, respectively.^{14e} MP3(FC)/6-31G**//RHF/6-31G* calculations^{14d} predict an activation barrier of 22.3 kcal/mol for the Diels–Alder cycloaddition of **2** to **3**, in excellent agreement with the experimental barrier^{7a} of 22.5 kcal/mol. Both BLYP/6-31G** and the Becke3LYP hybrid HF-DFT functional with 6-31G* and 6-31G** basis sets also give activation barriers for the concerted pathway in very good agreement with experiment.^{14a,b}

To date, there have been very few ab initio studies of diradical mechanisms in Diels–Alder¹⁵ or retro-Diels–Alder reactions,

(13) Wilsey, S.; Houk, K. N.; Zewail, A. H. *J. Am. Chem. Soc.*, in press.

(14) (a) Jursic, B. S. *J. Mol. Struct. (THEOCHEM)* **1995**, 358, 139. (b) Jursic, B. S.; Zdravkovski, Z. *J. Chem. Soc., Perkin Trans. 2* **1995**, 1223. (c) Jursic, B. S.; Zdravkovski, Z. *J. Mol. Struct. (THEOCHEM)* **1994**, 309, 249. (d) Jorgensen, W. L.; Lim, D.; Blake, J. F. *J. Am. Chem. Soc.* **1993**, 115, 2936. (e) Houk, K. N.; Li, Y.; Evanseck, J. D. *Angew. Chem., Int. Ed. Engl.* **1992**, 31, 682. (f) Houk, K. N.; Loncharich, R. J.; Blake, J. F.; Jorgensen, W. L. *J. Am. Chem. Soc.* **1989**, 111, 9172.

(15) (a) Goldstein, E.; Beno, B.; Houk, K. N. *J. Am. Chem. Soc.* **1996**, 118, 6036 and references therein. (b) Li, Y.; Houk, K. N. *J. Am. Chem. Soc.* **1993**, 115, 7478. (c) Bernardi, F.; Bottoni, A.; Field, M. J.; Guest, M. F.; Hillier, I. H.; Robb, M. A.; Venturini, A. *J. Am. Chem. Soc.* **1988**, 110, 3050. (d) Townshend, R. E.; Ramunni, G.; Segal, G.; Hehre, W. J.; Salem, L. *J. Am. Chem. Soc.* **1976**, 98, 2190.

(11) (a) Doering, W. v. E.; Roth, W. R.; Breuckmann, R.; Figge, L.; Lennartz, H.-W.; Fessner, W.-D.; Prinzbach, H. *Chem. Ber.* **1988**, 121, 1. (b) Doering, W. v. E.; Sachdev, K. *J. Am. Chem. Soc.* **1974**, 96, 1168.

(12) (a) Zewail, A. H. *J. Phys. Chem.* **1996**, 100, 12701. (b) Polanyi, J. C.; Zewail, A. H. *Acc. Chem. Res.* **1995**, 28, 119.

due to the large computational expense of most methods capable of a balanced treatment of closed- and open-shell species. Both dynamical and nondynamical correlation must be considered, and methods which do so (e.g. CASPT2¹⁶) are computationally intensive.

The [1,3] Sigmatropic Rearrangement. Bicyclo[3.2.0]hept-2-ene, **4**, undergoes a [1,3] sigmatropic rearrangement to form **1** with an activation barrier of 41.9 ± 4.5 kcal/mol.¹⁷ The two Woodward–Hoffmann allowed pathways for this reaction are the antarafacial-retention (*ar*) and suprafacial-inversion (*si*) routes.¹ The former is geometrically precluded, and the reaction is expected to occur with inversion of stereochemistry at the migrating carbon.

In a classic study of the rearrangements of substituted bicyclo[3.2.0]hept-2-enes, Berson demonstrated that the reactions of systems bearing an *exo* substituent on the migrating carbon occur by the *si* mechanism, in accordance with orbital symmetry predictions.¹⁸ He later showed that the allowed *si* pathway could be sterically blocked by substituents in the *endo* position on the migrating carbon, resulting in predominant retention of configuration (*sr*).¹⁹ The preference for the forbidden product led Berson and Salem to propose that “subjugent orbital” control causes the forbidden pathway to occur more easily than the stepwise paths.²

More recently, Baldwin and Belfield²⁰ and Klärner and co-workers^{3a} independently examined the rearrangements of **4**, deuterated at various positions, and observed product formation with predominant inversion of configuration (*si*) at the migrating carbon. However, up to 24% of the retention product (*sr*) was also obtained.

An orbital symmetry-allowed concerted mechanism has been ascribed to the *si* pathway.^{2,3,6,18–20} However, there have been several alternatives proposed for the formation of the *sr* product.^{2,3,6} One possibility is a stepwise reaction involving an equilibrated diradical intermediate which can form both *si* and *sr* products which competes with the concerted *si* mechanism. Alternatively, the diradical intermediate might close to the *sr* product before rotation about the terminal methylene can occur. Finally, Berson⁶ suggested that the *sr* product could be formed via an orbital symmetry-forbidden concerted mechanism which is energetically more favorable than a diradical route, as a result of “subjugent orbital” stabilization² of the transition structure.

Carpenter studied the [1,3] sigmatropic rearrangement of **4** to **1** using AM1 and PM3 semiempirical direct dynamics techniques.⁵ On the semiempirical surfaces, diradical intermediates are separated from the reactants and products by barriers of 2–8 kcal/mol. The dynamics calculations predict two separate intermediate populations. One has a very short lifetime (~250–350 fs) and leads exclusively to product with inversion of stereochemistry at the migrating carbon. Here, the dynamics of motion cause concerted movement to the inverted product without pausing to equilibrate the stereochemistry. The other intermediate has a much longer lifetime and may result in both inversion and retention of stereochemistry in the product.

Computational Methodology

The potential energy surfaces for both the retro-Diels–Alder reaction of **1** and the [1,3] sigmatropic rearrangement of **4** to **1** were explored with the Becke3LYP²¹ hybrid HF-DFT method and using the 6-31G*

Table 1. Becke3LYP/6-31G* Relative Energies, Enthalpies (298.15 K), Entropies, $\langle S^2 \rangle$ Values, and Singlet–Triplet Separations for Structures 1–16^a

	E_{rel} (kcal/mol)	H_{rel} (kcal/mol)	S_{rel} (eu)	$\langle S^2 \rangle$	ΔE_{ST}^b
norbornene (1)	0.0	0.0	0.0	0.00	
cyclopentadiene + ethylene (2 + 3)	18.4	20.3	44.7	0.00	
bicyclo[3.2.0]hept-2-ene (4)	5.4	5.8	3.0	0.00	
concerted T. S. (5)	40.8	41.3	4.0	0.00	
diradical T. S. 1 (6)	53.2	54.2	8.2	0.99	1.3
diradical intermediate (7)	48.1	49.7	12.6	1.02	0.6
diradical T. S. 1 (8)	53.0	54.1	9.5	1.01	0.5
diradical intermediate (9)	48.1	49.6	12.4	1.01	0.6
diradical T. S. 2 (10)	52.8	53.9	8.9	0.62	11.9
diradical T. S. 2 (11)	53.5	54.7	8.9	0.62	11.9
diradical T. S. (12)	51.4	52.5	9.6	1.02	0.3
diradical intermediate (13)	48.3	50.0	14.4	1.03	0.1
diradical T. S. (14)	50.5	51.4	7.0	0.85	6.1
diradical (15)	48.3	49.8	11.8	1.02	0.4
diradical T. S. (16)	49.2	50.4	10.0	1.03	−0.1

^a Entropies and thermal corrections to enthalpies calculated from unscaled vibrational frequencies. E_{rel} values include corrections for zero-point vibrational energy. ^b ΔE_{ST} = energy of triplet minus energy of spin-contaminated singlet, in kcal/mol at singlet geometry.

basis set.²² Restricted (RBecke3LYP) and unrestricted (UBecke3LYP) wave functions were used for closed- and open-shell species, respectively.

While there are some concerns regarding the use of DFT which stem from the lack of exact functionals,²³ we have found that the Becke3LYP/6-31G* method predicts activation barriers for closed- and open-shell pathways of pericyclic reactions in excellent agreement with available experimental data.^{15a,24} Excellent energies of reaction are obtained as well. Both concerted and diradical mechanisms for the butadiene/ethylene Diels–Alder reaction have been studied at the Becke3LYP/6-31G* level,^{15a} and an “energy of concert”¹¹ of 2–7 kcal/mol is predicted for the reaction, in excellent agreement with the best thermochemical estimates^{10,11} and QCISD(T)/6-31G**/CASSCF/6-31G* calculations.^{15b} In addition, the potential surface for the vinylcyclopropane to cyclopentene rearrangement has been explored with both Becke3LYP/6-31G* and CASSCF/6-31G* calculations.²⁵ For this reaction, which occurs in a single step with a diradical transition state, both methods predict very similar energetics.

The Becke3LYP/6-31G* wave functions for the open-shell species in this study all exhibit some degree of spin contamination, with $\langle S^2 \rangle$ values ranging from 0.62 to 1.03 (Table 1), since these wave functions are not pure eigenfunctions of the S^2 operator.²⁶ Single points were also computed for the triplet states of open-shell species in order to assess the effect of this spin contamination on the singlet energies. The role of spin contamination is discussed later in the paper.

All calculations were carried out with Gaussian 94.²⁷ Structures **1–16** were fully optimized with the exception of the diradical **15** for which all convergence criteria except the rms displacements fell below the threshold values. The failure of the rms displacements to converge is a result of the extremely flat potential surface in the vicinity of the structure. For several of the structures, the optimization step-sizes were decreased to facilitate location of the stationary points. Vibrational frequency calculations were performed on all stationary points, and

(21) (a) Becke, A. D. *J. Chem. Phys.* **1993**, *98*, 5648. (b) Lee, C.; Yang, W.; Parr, R. G. *Phys. Rev. B* **1988**, *37*, 785.

(22) Hehre, W. J.; Radom, L.; Schleyer, P. v. R.; Pople, J. A. *Ab Initio Molecular Orbital Theory*; Wiley: New York, 1986.

(23) Wiest, O.; Montiel, D. C.; Houk, K. N. *J. Phys. Chem. A* **1997**, *101*, 8378.

(24) Houk, K. N.; Beno, B. R.; Nendel, M.; Black, K.; Yoo, H. Y.; Wilsey, S.; Lee, J. K. *J. Mol. Struct. (THEOCHEM)* **1997**, *398–399*, 169.

(25) (a) DFT: Houk, K. N.; Nendel, M.; Wiest, O.; Storer, J. W. *J. Am. Chem. Soc.* **1997**, *119*, 10545. (b) CASSCF: Davidson, E. R.; Gajewski, J. *J. Am. Chem. Soc.* **1997**, *119*, 10543.

(26) (a) Pople, J. A.; Gill, P. M. W.; Handy, N. C. *Int. J. Quantum Chem.* **1995**, *56*, 303. (b) Baker, J.; Scheiner, A.; Andzelm, J. *Chem. Phys. Lett.* **1993**, *216*, 380.

(16) (a) Andersson, K.; Malmqvist, P. A.; Roos, B. O.; Sadlej, A. J.; Wolinski, K. *J. Phys. Chem.* **1990**, *94*, 5483. (b) Andersson, K.; Malmqvist, P. A.; Roos, B. O. *J. Chem. Phys.* **1992**, *96*, 1218.

(17) Cocks, A. T.; Frey, H. M. *J. Chem. Soc. A* **1971**, 2564.

(18) Berson, J. A.; Nelson, G. L. *J. Am. Chem. Soc.* **1967**, *89*, 5503.

(19) Berson, J. A.; Nelson, G. L. *J. Am. Chem. Soc.* **1970**, *92*, 1096.

(20) Baldwin, J. E.; Belfield, K. D. *J. Am. Chem. Soc.* **1988**, *110*, 296.

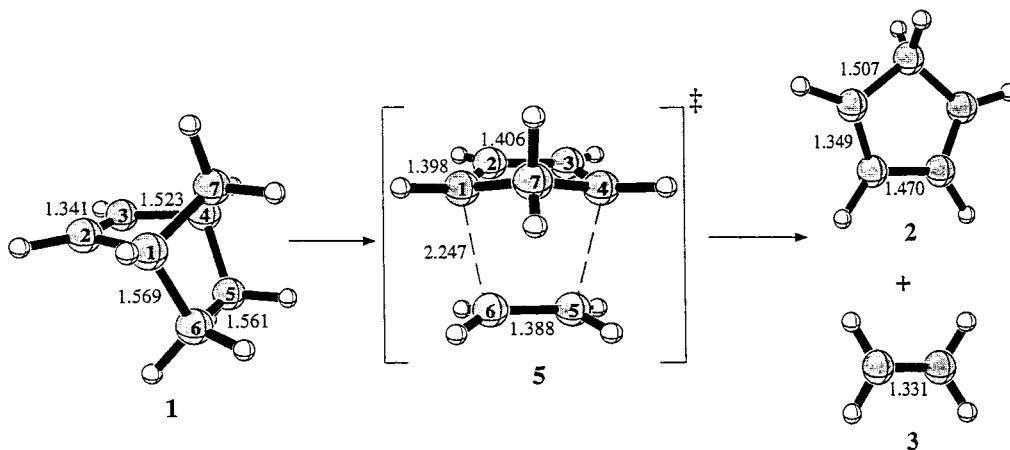


Figure 2. Becke3LYP/6-31G* optimized reactant, **1**, concerted transition structure, **5**, and products, **2** and **3** of the retro-Diels–Alder reaction of norbornene. All bond lengths are in Å.

transition structures were characterized by a single imaginary frequency, whereas reactants, intermediates, and products had none. Primary ¹³C kinetic isotope effects were calculated with the program QUIVER²⁸ from vibrational frequencies scaled by 0.963.²⁹

Results and Discussion

The Norbornene Retro-Diels–Alder Reaction. The Becke-3LYP/6-31G* optimized reactant **1**, concerted transition structure **5**, and products of the retro-Diels–Alder reaction of norbornene (**2** and **3**) are shown in Figure 2. The concerted transition structure for this reaction, calculated at several theoretical levels¹⁴ including Becke3LYP/6-31G*,^{14a} has been reported previously. The geometry of the synchronous concerted transition structure **5** is similar to that of **1** (Figure 2). The largest structural difference is a 0.68 Å increase in the lengths of the breaking C1–C6 and C4–C5 bonds in transition structure **5** relative to the lengths of the fully formed bonds in **1**. The C1–C2 and C3–C4 bonds have decreased in length by 0.13 Å, and the length of the C5–C6 bond has decreased by 0.17 Å in **5**. The breaking C–C bonds in transition structure **5** are about 0.03 Å shorter than those in the synchronous concerted transition structure for the retro-Diels–Alder reaction of cyclohexene, calculated at the same level.^{15a} The cyclohexene reaction is more endothermic and consequently has a later transition state.

Norbornene can also undergo a retro-Diels–Alder reaction through a diradical mechanism (Figure 1). The first step of this mechanism involves cleavage of the C1–C6 (or C4–C5) bond, through either transition state **6** leading to the “anti” intermediate **7**, or through transition state **8** leading to the “gauche-out” intermediate **9**. Despite extensive searches, a “gauche-in” intermediate, where the C3–C4–C5–C6 torsional angle is about 60°, has not been located. This is not surprising since closure of this hypothetical species to norbornene would have essentially no barrier. The intermediates **7** and **9** can either (1) close to reform norbornene (**2**) equilibrate, or (3) fragment to form cyclopentadiene and ethylene. The diradical transition

structures and intermediates for these mechanistic alternatives are shown in Figure 3.

In the transition structures **6** and **8**, the C1–C6 bond is completely broken. The distances between C1 and C6 are 3.86 and 4.42 Å, respectively. Animation of the imaginary frequencies corresponding to motion along the reaction coordinate in both cases shows primarily rotation about the C4–C5 bond. Formation of both the anti and gauche-out diradicals **7** and **9** is endothermic, and thus **6** and **8** are geometrically very similar to **7** and **9**, in accordance with the Hammond postulate.³⁰

The intermediates **7** and **9** both contain an allyl radical moiety (C1–C2–C3) and a methylene radical center at C6. Structurally, these intermediates are very similar to those found along the diradical pathway of the cyclohexene retro-Diels–Alder reaction at the same level of theory.^{15a}

Direct bond breakage in the intermediates **7** and **9**, through the transition structures **10** and **11**, leads to cyclopentadiene and ethylene. The breaking C4–C5 bonds in the transition structures **10** and **11** are elongated by 0.29 and 0.30 Å, respectively, relative to their lengths in the intermediates **7** and **9**. No transition structure for direct equilibration of the anti and gauche-out intermediates was located, despite several attempts. However, a diradical transition structure **12**, with a twisted methylene group was located. This transition structure connects anti and gauche-out diradicals with similarly twisted methylene groups. The twisted anti intermediate **13** was fully optimized, but the maximum displacements at the twisted gauche-out intermediate could not be converged since the eigenvalue corresponding to methylene torsion is so small.

The anti diradical **13** differs from **7** only in the conformation of the C6–methylene moiety, which is rotated by approximately –120° about the C5–C6 bond. In fact, there are three possible conformations the methylene can adopt; the third would be obtained by rotating by +120°. In theory, these three conformations will exist for all the diradical species formed after the C1–C6 bond has broken; however, in practice the barrier for rotating the methylene group is so small that many of these conformations are not stable structures on the potential energy surface. Both the transition structure for equilibration between **7** and **9** and the twisted gauche-out intermediate are examples of these.

Energetics of the Norbornene Retro-Diels–Alder Reaction. An energy profile for the retro-Diels–Alder reaction of norbornene is shown in Figure 4. Relative energies include zero-point energy corrections. The DFT calculations predict a ΔE_{rxn}

(27) *Gaussian 94* (Revision C.2), Frisch, M. J.; Trucks, G. W.; Schlegel, H. B.; Gill, P. M. W.; Johnson, B. G.; Robb, M. A.; Cheeseman, J. R.; Keith, T. A.; Petersson, G. A.; Montgomery, J. A.; Raghavachari, K.; Al-Latham, M. A.; Zakrzewski, V. G.; Ortiz, J. V.; Foresman, J. B.; Cioslowski, J.; Stefanov, B. B.; Nanayakkara, A.; Challacombe, M.; Peng, C. Y.; Ayala, P. Y.; Chen, W.; Wong, M. W.; Andres, J. L.; Replogle, E. S.; Gomperts, R.; Martin, R. L.; Fox, D. J.; Binkley, J. S.; Defrees, D. J.; Baker, J.; Stewart, J. J. P.; Head-Gordon, M.; Gonzalez, C.; Pople, J. A. Gaussian, Inc.: Pittsburgh, PA, 1995.

(28) Saunders, M.; Laidig, K. E.; Wolfsberg, M. *J. Am. Chem. Soc.* **1989**, *111*, 8989.

(29) Rauhut, G.; Pulay, P. *J. Chem. Phys.* **1995**, *99*, 3093.

(30) Hammond, G. S. *J. Am. Chem. Soc.* **1955**, *77*, 334.

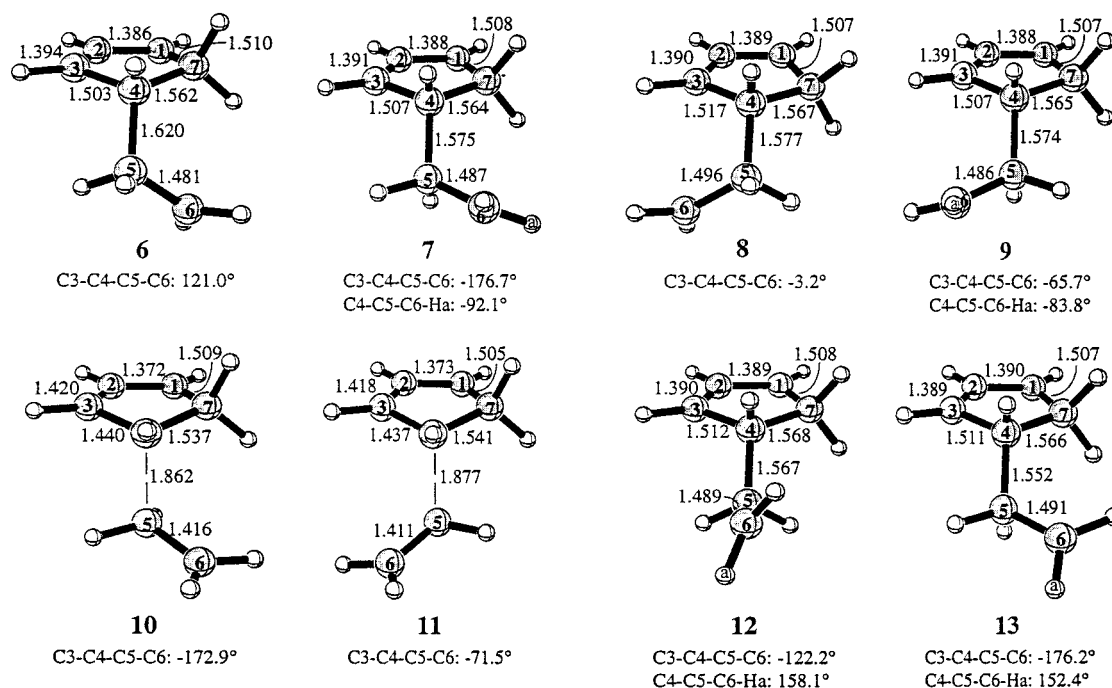


Figure 3. Becke3LYP/6-31G* optimized diradical transition structures (6, 8, 10, 11, and 12) and intermediates (7, 9, and 13) on the norbornene retro-Diels-Alder potential energy surface. All bond lengths are in Å.

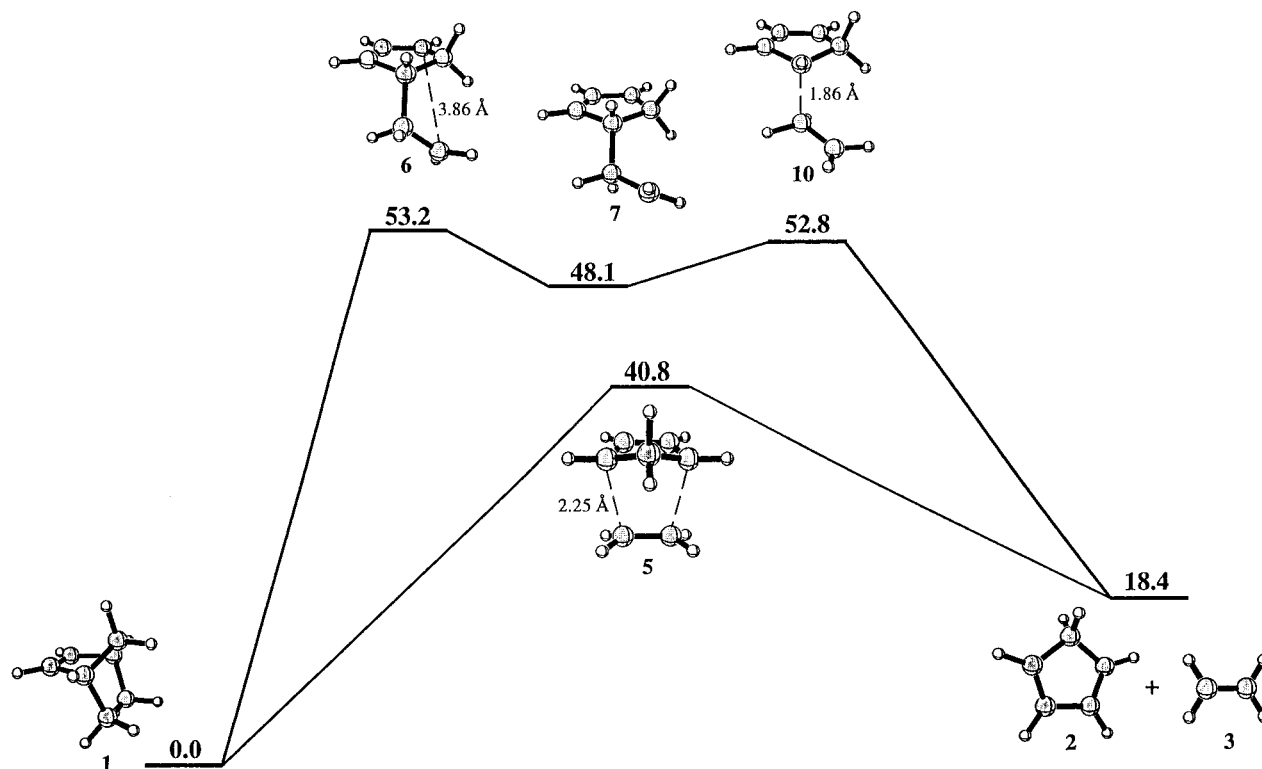


Figure 4. Energy diagram for the retro-Diels-Alder reaction of 1. Energies are in kcal/mol and include zero-point corrections.

of 18.4 kcal/mol. The ΔE^\ddagger for the concerted pathway is 40.8 kcal/mol. This is 20.6 kcal/mol less than that predicted for the retro-Diels-Alder reaction of cyclohexene at the same level of theory.^{15a}

The lowest energy stepwise mechanism is through the anti intermediate 7, and this is the pathway shown in the figure. The rate-determining step of this mechanism involves breaking the C1-C6 bond via transition structure 6. The ΔE^\ddagger is 53.2 kcal/mol; therefore, the DFT calculations predict that the concerted pathway for the retro-Diels-Alder reaction of 1 is

favored over the stepwise anti diradical route by 12.4 kcal/mol. The energy of the anti intermediate, 7, is 48.1 kcal/mol above that of norbornene. This is in excellent agreement with the 48 kcal/mol predicted by Benson.¹⁰ Fragmentation of 7 into cyclopentadiene and ethylene occurs through transition structure 10 with a barrier of 4.7 kcal/mol.

The rate-determining step in the gauche-out stepwise mechanism is fragmentation of the intermediate 9 through transition state 11, which makes the overall barrier for this mechanism 0.3 kcal/mol higher in energy than that for the anti mechanism.

The barrier for formation of a twisted gauche-out intermediate from the twisted anti intermediate **13**, through transition structure **12**, is 3.1 kcal/mol. The twisted anti intermediate **13** lies only 0.2 kcal/mol higher in energy than the anti intermediate **7**, with only a facile methylene rotation separating the two structures. Therefore, the barrier for equilibration of the anti and gauche-out intermediates **7** and **9** can be estimated to be 3.3 kcal/mol. This is 1.4 kcal/mol lower than the barrier for cleavage of **7** to form cyclopentadiene and ethylene and 1.8 kcal/mol lower than for collapse of **7** to norbornene. However, the barrier for fragmentation of the gauche-out intermediate **9** is 0.7 kcal/mol higher than that for fragmentation of **7**, such that **9** will preferentially close to norbornene rather than fragment. Therefore, the anti and gauche-out diradicals will equilibrate, but formation of cyclopentadiene and ethylene will occur primarily through the anti intermediate **7**.

The relative enthalpies and entropies of the stationary points on the norbornene retro-Diels–Alder potential energy surface are listed in Table 1. The ΔH^\ddagger for the concerted pathway is 41.3 kcal/mol. This underestimates the experimental ΔH^\ddagger by only 2.2 kcal/mol.⁸ For the diradical mechanism, the ΔH^\ddagger is 54.2 kcal/mol.

The wavefunctions for structures **6–9** are all approximately 50% singlet:50% triplet, and the singlet and triplet are nearly degenerate (Table 1). Consequently, the UB3LYP energies and geometries should be reasonable for these species. The spin contamination in **10** and **11** is lower, as the diradicals are cleaving to closed-shell species. These barriers are likely to be overestimated because of significant admixture of higher energy triplet states. Clearly, even when taking into account the effects of spin contamination, there is a strong enthalpic preference for the concerted pathway.

The ΔH_{rxn} is predicted to be 20.3 kcal/mol in good agreement with the 23.2 kcal/mol value from experiment.⁹ DFT calculations predict ΔS^\ddagger values of 4.0 and 8.2 eu for the concerted and anti diradical pathways, respectively. The ΔS^\ddagger predicted for the concerted pathway is within 0.5 eu of the experimental ΔS^\ddagger ,⁸ while that for the diradical mechanism is more than 5 kcal/mol too positive. A ΔS_{rxn} of 46.0 eu is predicted by the DFT calculations.

The Becke3LYP/6-31G* enthalpy and entropy of activation for the concerted pathway of the norbornene retro-Diels–Alder reaction are in excellent agreement with experimental data,⁸ while both quantities for the diradical mechanism differ significantly from the experimental results. This provides strong support for a concerted mechanism.

Comparison of Predicted and Experimental ¹³C Primary Kinetic Isotope Effects. Recent work by Singleton and Thomas has provided a technique for the measurement of high-precision KIEs.³¹ The precision of these experimentally determined KIEs is sufficient to allow differentiation between similar reaction mechanisms, where previously, KIE results were often ambiguous. We have shown that Becke3LYP/6-31G* calculations predict both ²H and ¹³C KIEs for the Diels–Alder reaction of isoprene with maleic anhydride in excellent agreement with high-precision experimental results.³²

High-precision ¹³C primary KIEs for the retro-Diels–Alder reaction of **1** have been measured.³³ These are listed in Table 2, along with Becke3LYP/6-31G* predicted KIEs. The KIEs predicted for the retro-Diels–Alder reaction occurring through

Table 2. Becke3LYP/6-31G* and Singleton's Experimental³³ ¹³C Primary Kinetic Isotope Effects (493.15 K) for the Retro-Diels–Alder Reaction of Norbornene^a

	KIE			experimental
	concerted T. S. (5)	diradical T. S. (6)	diradical T. S. (10)	
C1– ¹³ C	1.014	1.004	1.003	1.014 ± 0.001
C2– ¹³ C	1.001	1.002	1.001	1.000
C3– ¹³ C	1.001	1.006	1.006	1.000
C4– ¹³ C	1.014	1.002	1.025	1.014 ± 0.001
C5– ¹³ C	1.017	1.008	1.028	1.014 ± 0.001
C6– ¹³ C	1.017	1.020	1.010	1.014 ± 0.001
C7– ¹³ C ^b	1.000	1.000	1.000	1.000

^a Vibrational frequencies used in KIE calculations were scaled by 0.963. ^b All KIEs are scaled relative to the C7 value which is assumed to be 1.000.

the concerted transition structure **5** are in excellent agreement with the experimental results.

Since both transition structures along the anti stepwise retro-Diels–Alder pathway are similar in energy, KIEs were calculated for two possible alternatives, one in which passage through transition structure **6** is the rate-determining step and another where passage through transition structure **10** is rate-determining. In both cases, there is poor agreement between the measured and predicted KIEs.

The excellent agreement between the measured KIEs and those predicted for the concerted pathway provides further support for a concerted mechanism for the retro-Diels–Alder reaction of **1**.

The [1,3] Sigmatropic Rearrangement of Bicyclo[3.2.0]hept-2-ene to Norbornene. A careful search of the potential energy surface for the rearrangement of **4** to **1** gave the reaction surface shown in Figure 5, along with the retro-Diels–Alder surfaces for comparison. The C1–C7 bond cleavage in **4** involves transition structure **14** and leads to a broad plateau on the potential energy surface. From this plateau, two possibilities exist for formation of **1**. A direct barrierless route leading to **1** with inversion of stereochemistry at C7 ([1_i, 3_s] shift), and an alternative pathway leading to the retention product ([1_r, 3_s] shift). No additional barrier was found separating **14** from norbornene.

Becke3LYP/6-31G* optimized geometries of the stationary points on the potential energy surface are shown in Figure 6. The energy of the diradical transition structure **14** is 45.1 kcal/mol above that of **4**. In **14**, the length of the breaking C1–C7 bond (2.589 Å) is 1.03 Å longer than the fully formed C1–C7 bond in reactant **4**. The lengths of forming or breaking C–C bonds in diradical transition structures for pericyclic reactions typically fall in the range of 1.8–2.0 Å.^{14,15} Transition structure **14** is a true diradical transition structure with an $\langle S^2 \rangle$ of 0.85. Because the pure triplet is 6 kcal/mol higher in energy, the energy of **14** will be overestimated somewhat by the UB3LYP results. In **14**, the C3–C7 distance is 3.694 Å. There is no interaction between these two centers.

Since there is no bonding at C3, the direction of rotation must result from repulsive interactions between the front lobe of the p orbital at C7 and the π orbital of the C2–C3 bond. Such an effect has been noted previously in another [1,3] shift, the vinylcyclopropane–cyclopentene rearrangement.^{25a} This motion leads to inversion of configuration at C7 and has already occurred to a significant extent in the transition state. However, the rotation is insufficient to allow interaction between the back lobe of the C7 p orbital and the C3 terminus of the allyl moiety which is expected for a concerted transition structure. The

(31) Singleton, D. A.; Thomas, A. A. *J. Am. Chem. Soc.* **1995**, *117*, 9357.

(32) Beno, B. R.; Houk, K. N.; Singleton, D. A. *J. Am. Chem. Soc.* **1996**, *118*, 9984.

(33) Singleton, D. A., private communication.

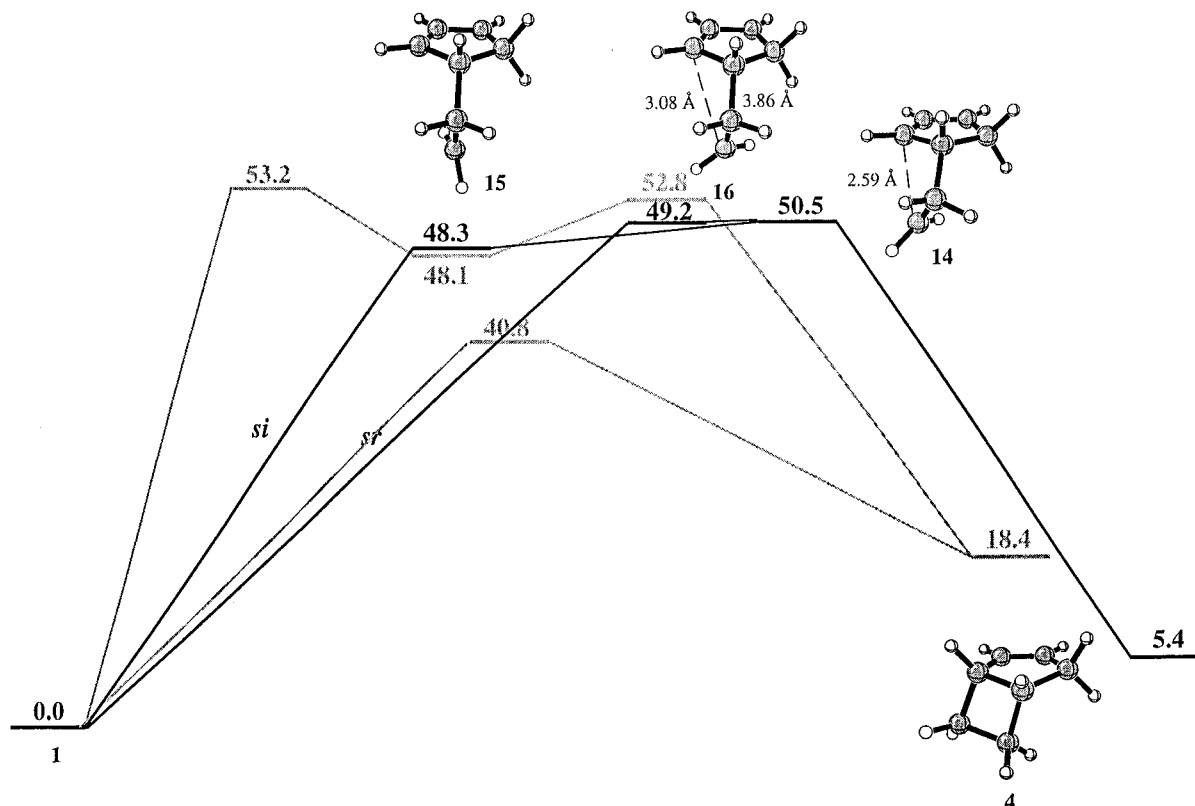


Figure 5. Becke3LYP/6-31G* energy profile for the [1,3] sigmatropic rearrangement of **4**. Energy profiles for the concerted and stepwise retro-Diels–Alder reactions are shown (in gray) for comparison. Energies are in parentheses, include zero-point corrections, and are given in kcal/mol.

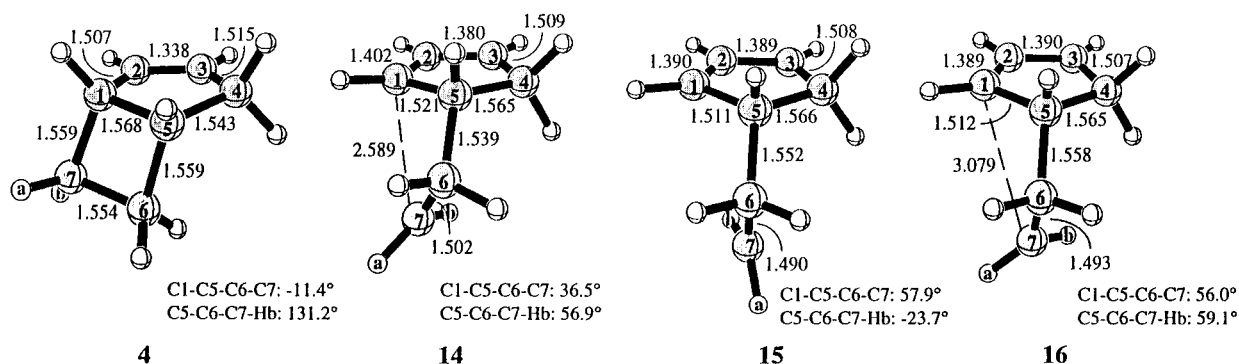


Figure 6. Becke3LYP/6-31G* optimized geometries for species on the potential energy surface for the [1,3] sigmatropic rearrangement of **4**. All bond lengths are in Å.

direction of rotation of C7 is consistent with that required for the orbital symmetry allowed *si* reaction,¹⁹ even though there is no cyclic conjugation in the transition state.

An intrinsic reaction coordinate (IRC) calculation was performed starting from transition structure **14** (open circles in Figure 7). The reaction coordinate led in one direction to **4**. In the other direction, a plateau lying 2.2 kcal/mol below **14** in energy was reached. Several attempts to complete the IRC failed due to the near zero slope of the potential energy surface. No fully optimized intermediate could be located in the flat region of the potential energy surface. However, a partially optimized diradical structure was obtained (**15**, Figure 6). For this structure, three of the four optimization convergence criteria fell below the threshold values.

Structure **15** is similar to transition structure **14**. The geometries of the five-membered rings are virtually identical in the two structures. However, in **15**, the C7 methylene moiety has rotated to larger degree than in **14** and is nearly perpen-

dicular to the plane of the cyclopentene ring. The allyl radical moiety and terminal methylene radical are orthogonal, and interaction between the two centers is minimal. The energy of **15** is 2.2 kcal/mol below that of transition structure **14**.

To map more of the potential energy surface for the [1,3] sigmatropic rearrangement of **4** to **1**, a series of partial geometry optimizations starting from **1** and **4** were performed. For those starting from **4**, the C1–C7 bond length was increased in small increments. Likewise, the C4–C5 bond length was varied in the constrained optimizations starting from **1**. As the C1–C7 bond is stretched in **4**, a maximum is reached, for which the energy and geometry correspond closely to those of transition structure **14**. However, no maximum is observed when the length of the C4–C5 bond in **1** is increased. In this case, the energy profile is best described as a broad shoulder.

When the two energy profiles are plotted together, they form a smooth curve (Figure 7), and visualization of the partially optimized structures along the curve shows a continuous

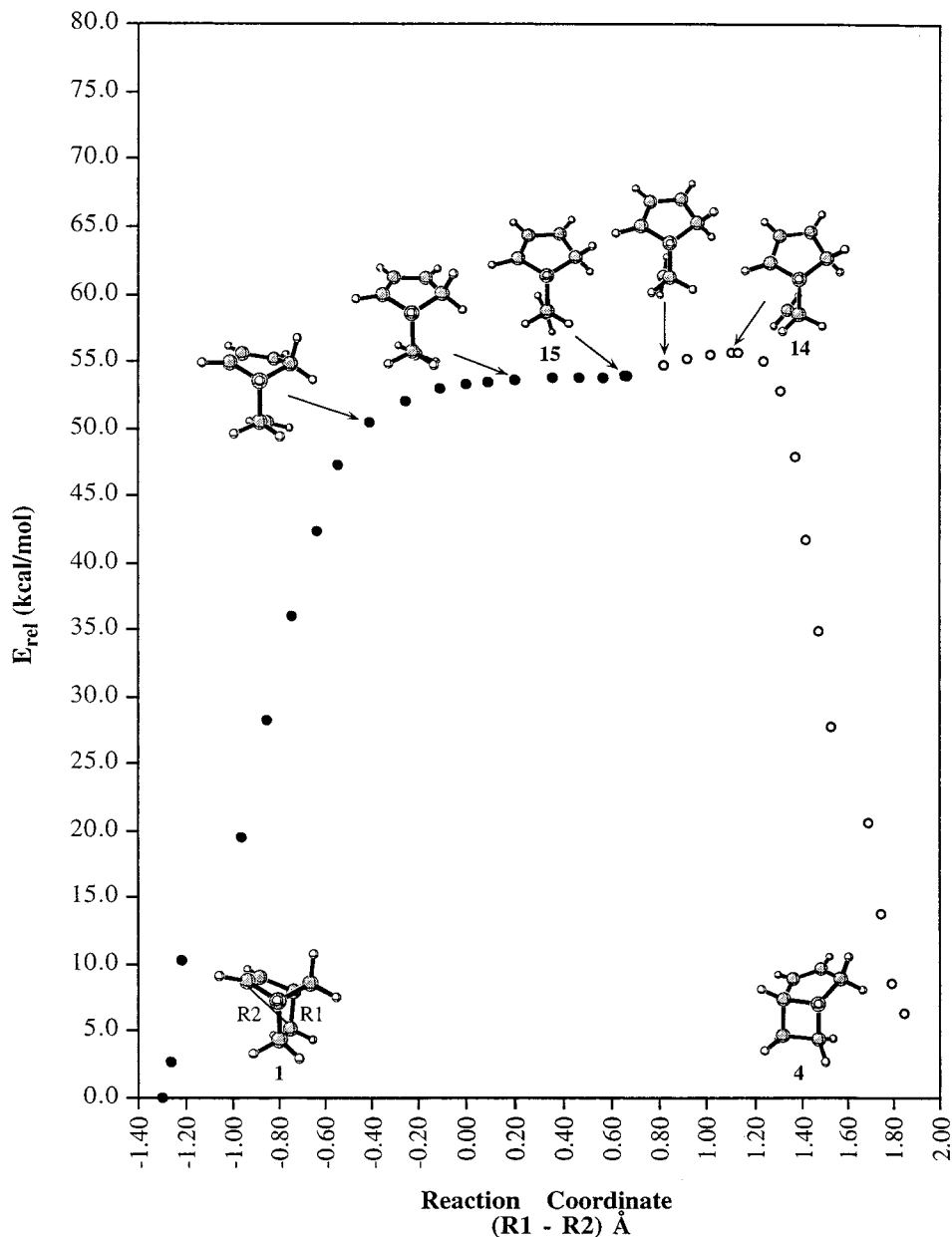


Figure 7. Becke3LYP/6-31G* partial IRC and energy profile for the [1,3] sigmatropic rearrangement of **4**.

progression from **1** to **4** with concomitant rotation of the migrating methylene moiety. The energy profile in Figure 7 closely resembles the IRC obtained for the vinylcyclopropane to cyclopentene rearrangement.²⁵

Another authentic transition structure (**16**) was located which is structurally similar to **15**, but higher in energy. The potential surface in the vicinity of this transition structure is quite flat ($\nu_i = 151.8i$), and attempts to follow the reaction path downhill with IRC calculations were unsuccessful. Geometry optimizations started from this transition structure led in our calculations to **1**, and in those of a reviewer to **4**. Visualization of the imaginary frequency for this transition structure shows almost exclusive rotation about the C6–C7 bond. The ZPE-corrected energy of **16** is 49.2 kcal/mol, only 0.9 kcal/mol above **15**. In this pure diradical, the singlet and triplet are degenerate, and therefore spin projection is not expected to change the energy of this species. This is a transition structure for rotation about C6–C7 in the opposite direction to that leading to *si* product. Starting from **16**, further rotation brings the front face of the

radical into interaction with the allyl radical terminus, and collapse to **1** with retention will occur from this species.

A reviewer proposed the following type of insightful analysis to convey the motions which occur on this surface. Figure 8 shows a plot of the torsional angle for C7H2 rotation versus the reaction coordinate, ΔR , which is $d(C7-C1) - d(C7-C3)$. The pathway passing through structures **4**, **14**, **15**, and **1**, leads to inversion, and the pathway via **4**, **14**, **16**, and **1'**, leads to retention. Structures **14** and **14'** are identical, or involve one 180° rotation with respect to the C₆–C₇ bond if C₇ is labeled with one deuterium; these are the highest transition structures found on this surface. From **14**, continued rotation about the C₆–C₇ bond leads to the lower energy plateau, containing structure **15**, and then on to **1** with inversion. Alternatively, from the vicinity of **14**, a slight dip in energy and then passage over a second transition structure **16** and on to **1'** will occur with retention of configuration. The situation is actually even more complex than implied here, since the methylene group pyramidalizes and inverts at some points on the surface. In terms

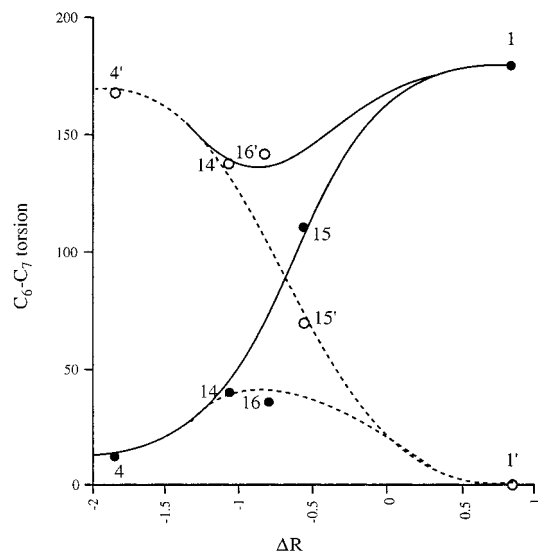


Figure 8. Contour plot of retention and inversion pathways from **4** via **16** and **15**, respectively, in terms of torsional angle for CH_2 rotation and the reaction coordinate, ΔR .

of bond length changes, the two processes are very similar and are closely related to the vinylcyclopropane surface we investigated earlier.²⁵ A quantitative explanation of the reaction stereochemistry will require consideration of dynamics, but it is clear that the inversion pathway involves a smooth and continuous rotation, whereas the retention pathway involves a reversal in rotational momentum, presumably a disfavored process.

The exact nature of the potential surface in the region of **14** and **16** has been difficult to determine because of the very similar energies of species with different values of R , $\text{C}_6\text{--C}_7$ rotation, and pyramidalization. The energetics of Figure 5 and torsional diagram of Figure 8, taken together, indicate that from transition state **14**, continuing the $\text{C}_6\text{--C}_7$ torsional motion in the same direction causes the most rapid decrease in energy and leads to the *si* product, while a reversal of the $\text{C}_6\text{--C}_7$ torsion results in only a slight decrease in energy and eventually to the *sr* product.

The Becke3LYP/6-31G* ΔH^\ddagger , ΔS^\ddagger , and ΔG^\ddagger (298 K) for the [1,3] shift of **4** to **1** are 45.6 kcal/mol, 4.0 eu, and 44.4 kcal/mol, respectively. For the reverse reaction, the predicted activation parameters are 51.4 kcal/mol, 7.0 eu, and 49.3 kcal/mol.

The shape of the potential surface for the [1,3] rearrangement of **4** to **1** predicted by DFT is quite different from that predicted by semiempirical methods.⁵ At the AM1 and PM3 levels of theory, the formation of **4** from a diradical intermediate occurs with barriers of 2.2 and 3.6 kcal/mol, respectively. No true intermediate is found at the Becke3LYP level, although the plateau on the potential energy surface is about 2 kcal/mol below the transition structure. For closure of the intermediate to **1**, the AM1 and PM3 activation barriers are 5.1 and 7.5 kcal/mol, respectively; in contrast, no barrier is found for the *si* pathway at the Becke3LYP/6-31G* level, and a barrier of less than 1 kcal/mol is predicted for back rotation about $\text{C}_6\text{--C}_7$, leading to the *sr* product. Carpenter proposed the concept of “dynamic matching” to explain how stereoselectivity could occur when AM1 and PM3 predict a relatively stable diradical that should completely scramble stereochemistry.⁵ Our results show that the shape of the surface is quite different from the semiempirical prediction, but dynamics are very important for the quantitative understanding of reactions occurring on such flat surfaces. Transition-state theory cannot provide predictions of stereo-

chemistries for such a surface, where the stereochemistry is determined after the rate-determining transition state and there are no significant intermediates.

Comparison of the Retro-Diels–Alder and [1,3] Sigma-Tropic Rearrangement Mechanisms. The energy of concert for the norbornene retro-Diels–Alder reaction is about 12 kcal/mol. Thus, the reaction should occur entirely via the concerted mechanism. However, several of the diradical stationary points are similar both structurally and energetically to those found on the [1,3] shift potential energy surface.

The partially optimized diradical structure from the plateau region of the [1,3] shift surface, **15**, and the anti intermediate, **7**, for the retro-Diels–Alder reaction are shown in Figure 9. Also shown is the last point (**17**) obtained in a relaxed scan of the retro-Diels–Alder potential surface in which the $\text{C}_3\text{--C}_4\text{--C}_5\text{--C}_6$ dihedral in the anti intermediate **7** was decreased incrementally. Attempts to continue the potential surface scan with the $\text{C}_3\text{--C}_4\text{--C}_5\text{--C}_6$ dihedral constrained to values less than 105° were unsuccessful because of a lack of convergence in the geometrical parameters.

Structures **7** and **15** are geometrically very similar. With the exception of the $\text{C}_4\text{--C}_5$ bonds, which differ by 0.023 Å, all of the $\text{C}_X\text{--C}_Y$ bonds in **15** are within 0.004 Å of their lengths in **7**. The most pronounced structural differences between the two structures are the dihedral angles about the $\text{C}_4\text{--C}_5$ and $\text{C}_5\text{--C}_6$ bonds. In **7**, the terminal methylene group projects away from the cyclopentadienyl ring, whereas it is centered under the ring in **15**. The plane defined by the terminal methylene group is approximately parallel to the plane of the ring in **7**, and nearly perpendicular in **15**. In **7** and **15**, the interactions between the methylene and allyl radical moieties are small as a consequence of the molecular geometry. The structural similarities of these two species are reflected in their energies, which differ by only 0.3 kcal/mol.

In structure **17**, the $\text{C}_4\text{--C}_7$ and $\text{C}_5\text{--C}_6$ bonds are nearly eclipsed, and the C_1 and C_6 radical centers are within about 3.4 Å of each other, whereas in **7** and **15**, this distance is greater than 3.7 Å. The $\text{C}_4\text{--C}_5$ bond in **17** is 0.062 and 0.085 Å longer than the corresponding bond in **7** and **15**, respectively. This elongation of the $\text{C}_4\text{--C}_5$ bond as the $\text{C}_1\text{--C}_6$ distance decreases suggests that the singlet diradical potential energy surface leading from the anti diradical intermediate **7** to norbornene may eventually intersect the vibrational well of the concerted retro-Diels–Alder transition structure at the turning point of an asymmetric vibration. The second real vibrational mode at the concerted transition structure involves a decrease in one of the forming C--C bond lengths, and a concomitant increase in the other, which should lead to a geometry similar to that of **17**.

The energy (uncorrected for ZPE) of **17** is 4.0 and 3.8 kcal/mol above those of **7** and **15**, respectively. This is higher than the eclipsed barrier in propane, but less than that in butane. The barrier between **7** and **15** is mainly torsional and steric in nature.

Potential energy profiles for the concerted pathway of the retro-Diels–Alder reaction of **1**, the [1*i*,3*s*] and [1*r*,3*s*] shifts of **1** to **4**, and the first step of the diradical mechanism for the retro-Diels–Alder reaction in the region of the concerted transition state are shown in Figure 10. For the concerted pathway the data points were taken from an IRC calculation, while those for the [1*i*,3*s*] shift were obtained from UBecke3LYP/6-31G* constrained optimizations of **1** in which the length of the breaking C--C bond was incrementally increased. The [1*r*,3*s*] transition structure, **16**, was obtained from a full

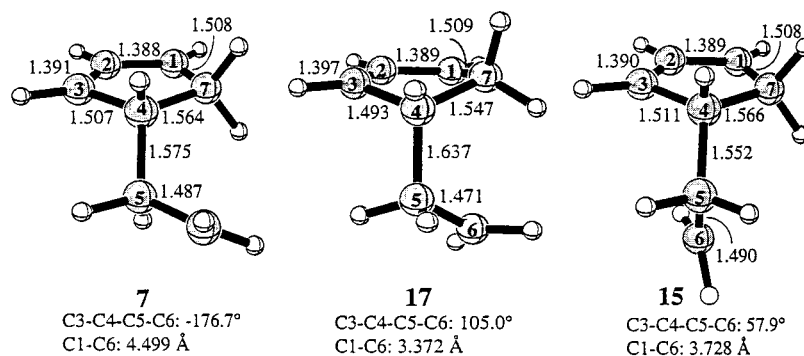


Figure 9. Comparison of retro-Diels–Alder and [1,3] shift diradical species **7**, **15**, and **17**.

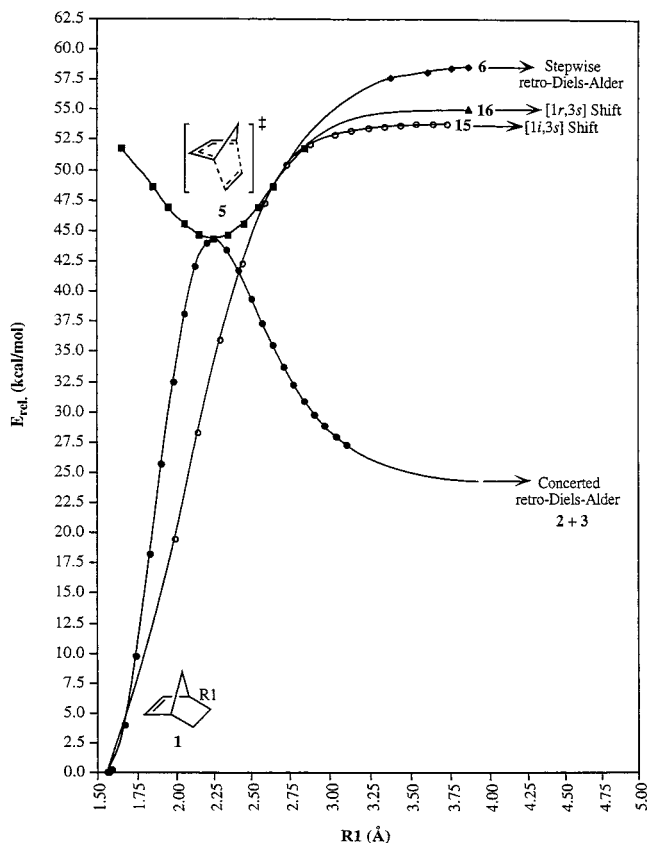


Figure 10. Becke3LYP/6-31G* potential energy profiles for the retro-Diels–Alder and [1,3] shift reactions of **1**. Energies are in kcal/mol and are not corrected for ZPE.

optimization. For the anti diradical retro-Diels–Alder pathway, the data points were obtained from UBecke3LYP/6-31G* constrained optimizations of **7** with the C3–C4–C5–C6 dihedral angle decreased incrementally. The portions of the potential energy profiles depicted with dashed lines are extrapolated.

Also shown in Figure 10 are the potential energy values for asynchronous motion of the concerted retro-Diels–Alder transition structure corresponding to the the second real vibrational mode. This was approximated with UBecke3LYP/6-31G* constrained optimizations in which one of the forming bonds in the concerted transition structure was shortened and one was elongated by the same increment.

It is quite difficult to put all of these species on a single diagram, since there are 45 degrees of freedom plus energies to graph! Nevertheless, Figure 10 shows schematically the relationship between norbornene, the concerted decomposition pathway, and various diradical species. Examination of Figure

10 provides several important details regarding the relationship between the retro-Diels–Alder and [1,3] shift reaction pathways. First, the lowest energy reaction pathway for norbornene is the closed-shell, concerted retro-Diels–Alder route. The next lowest energy alternative is the [1,3] shift. This reaction occurs via a diradical mechanism in which the C1–C6 bond is broken as C6 moves toward C3 with concomitant rotation of the C6 methylene moiety, and it is the lowest energy pathway for homolytic cleavage of either the C1–C6 or C4–C5 bond in **1**. This path has neither torsional nor steric problems. About the same in energy, but dynamically disfavored is the [1*r*,3*s*] mechanism. Finally, the diradical pathway for the retro-Diels–Alder reaction is several kcal/mol higher in energy, due to the torsional and steric problems which disfavor formation of the anti diradical intermediates.

The most striking feature of Figure 10 is the intersection of the potential energy profile for asymmetric motion of the concerted transition state and the potential energy profiles for the [1,3] shifts and stepwise retro-Diels–Alder reactions. This indicates that all of the diradical species can collapse to norbornene or fragment to cyclopentadiene and ethylene through the concerted transition structure. Formation of **15**, **16**, and **6** all involve cleavage of one bond, but different torsional motions.

The 1,3-Shift Mechanism. Our calculations have some bearing on Carpenter's dynamic matching treatment of this and related reactions.⁵ At the UB3LYP level, there is no diradical intermediate between norbornene and bicyclo[3.2.0]hept-2-ene. The lower energy transition structure, **14**, leads to a level surface, **15**, and to [1*i*, 3*s*] stereochemistry. About 1 kcal/mol higher in energy than **15**, a second transition structure, **16**, still lower in energy than **14**, results in overall [1*r*, 3*s*] stereochemistry. Simple stochastic behavior is unlikely for such a flat surface; the dynamic effects pointed out by Carpenter will influence product ratios. The semiempirical surfaces employed by Carpenter⁵ predict deep minima for diradical species. The qualitative picture which emerges from our calculations is of a competition between two processes; both involve diradical transition states with essentially no bonding between radical centers, and no stable diradical intermediates.

Conclusions

The retro-Diels–Alder reaction of **1** is predicted to occur via a closed-shell concerted mechanism, with two possible open-shell diradical routes about 12–13 kcal/mol higher in energy. The calculated activation parameters, enthalpy of reaction, and ¹³C primary kinetic isotope effects are in excellent agreement with experimental data.

For the [1,3] sigmatropic rearrangement, a concerted mechanism with a diradical transition structure proceeding through a

broad, flat region of the potential energy surface leads to the experimentally predominant *si* product. A second diradical transition structure corresponds to rotation about C6–C7 and subsequent closure to norbornene will occur with retention. The predicted activation barriers are in good agreement with the experimental values for these reactions.

Acknowledgment. We are grateful to the National Science Foundation for financial support of this research and to the National Center for Supercomputing Applications (NCSA) and

UCLA Office of Academic Computing for computer time. We thank Professor Ahmed Zewail for providing us with results before publication and for extensive discussions.

Supporting Information Available: Cartesian coordinates for structures **1–16** and tables of energies (PDF). This material is available free of charge via the Internet at <http://pubs.acs.org>.

JA9818250